IEICE TRANS. COMMUN., VOL.E88–B, NO.8 AUGUST 2005

PAPER Special Section of 2004 International Symposium on Electromagnetic Compatibility

Comparison of Site Attenuation Analysis Results between FDTD and Ray-Tracing Method Using Compact Anechoic Chamber

Masato KAWABATA[†a)], Yasuhiro ISHIDA[†], Kazuo SHIMADA[††], *and* Nobuo KUWABARA[†††], *Members*

SUMMARY The site attenuation is an important parameter to evaluate an anechoic chamber. The ray-tracing method has been applied to analyze it. However, the lowest applicable frequency has not been cleared. In this paper, the FDTD method has been applied to analyze the site attenuation of a compact anechoic chamber from 30 MHz to 250 MHz, and this has been compared with the calculated one by the ray-tracing method to evaluate the lowest frequency where the ray-tracing method could be applied. The compact anechoic chamber, where the absorbers are placed on the all walls, has been used for the calculation. For FDTD analysis, the dipole antenna and the absorber have been modeled by using the large cell, whose size is larger than the diameter of the antenna element. For verification, the site attenuation of a compact anechoic chamber has been measured and compared with the calculated values by the FDTD method and the ray-tracing method. As the results, the calculated values by the ray-tracing method have larger deviation than the ones by the FDTD method when the frequency is less than 180 MHz.

key words: *FDTD method, ray-tracing method, compact anechoic chamber, site attenuation*

1. Introduction

Recently, emission radiated from electric and electronic equipment has disturbed with surrounding radio communication. Therefore, the emission levels and testing method have been published by CISPR [1]. In order to pass the conformity test, emission level from EUT (Equipment under Test) must be mitigated below the defined limit. In many cases, preliminary test is performed in a compact anechoic chamber. However, it is difficult to make clear the relations among different test sites because, particularly in a compact anechoic chamber, reflection from the absorber much influences the test results.

In order to evaluate relations among test sites, it is useful to computationally analyze the site attenuation of anechoic chambers. The ray-tracing method has been utilized to this analysis [2], but it cannot be applied for evaluation in the low frequency where wavelength is longer than the size of the anechoic chamber. On the other hand, the FDTD method [3] has been developed to calculate the site attenuation from 30 MHz to 100 MHz [4]. The FDTD method can be applied to analyze the site attenuation at any frequency. However, the large computer power and long calculation time are needed. Therefore, it is important to use properly the FDTD method and the ray-tracing method according to frequency.

In this paper, the site attenuation of a compact anechoic chamber is calculated by both the FDTD method and the ray-tracing method. On the FDTD calculation, the large cell, whose size is larger than the diameter of the antenna element, is used to model the dipole antenna and the absorber. The calculated results are compared with the measured ones to estimate the frequency where we should change the calculation method.

2. Calculation of Site Attenuation of Compact Anechoic Chamber

In order to estimate the frequency where the calculation method should be changed from the FDTD method to the ray-tracing method, we should calculate the site attenuation. The calculation method by the ray-tracing method has been reported [2]. However, the calculation by the FDTD method is difficult because it needs the large computer power and calculation time. Recently, the method using the large cell, where the size is larger than the diameter of the antenna element, has been reported [4]. We can calculate the site attenuation by PC using this method. However, the method can only be applied at 100 MHz or less. Therefore, we investigate the FDTD modeling method to calculate the site attenuation more than 100 MHz.

The calculation model of the site attenuation is illustrated in Fig. 1. The compact anechoic chamber is covered with the absorber on the all walls. Ferrite tile and pyramidal ferrite are used as the absorber. The site attenuation is

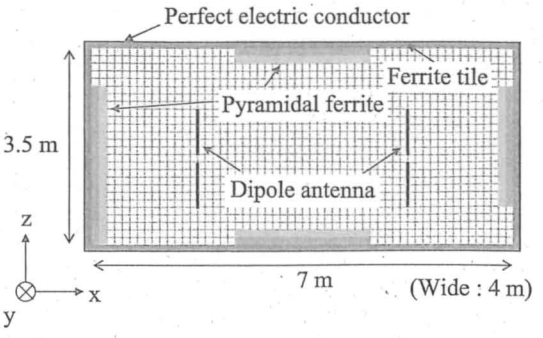

Fig. 1 FDTD analysis model of compact anechoic chamber.

Manuscript received November 18, 2004.
Manuscript revised March 14, 2005.

[†]The authors are with Fukuoka Industrial Technology Center, Kitakyushu-shi, 807-0831 Japan.
[††]The author is with Riken Eletech Corporation, Kumagaya-shi, 360-8522 Japan.
[†††]The author is with Kyushu Institute of Technology, Kitakyushu-shi, 804-8550 Japan.
a) E-mail: kawabata@fitc.pref.fukuoka.jp

DOI: 10.1093/ietcom/e88–b.8.3152

defined by the propagation characteristics between transmitting and receiving antenna in the anechoic chamber. Therefore, the site attenuation mainly depends on antenna characteristics and reflection from the absorber, so that the modeling of antennas and the absorber is very important.

2.1 FDTD Modeling of Antenna

Half-wave or tuned dipole antennas are generally used to evaluate the site attenuation of an anechoic chamber from 30 MHz to 1000 MHz [5]. However, these dipole antennas cannot be used in the compact anechoic chamber in the low frequency where the antenna element length is longer than the size of the chamber. Therefore, the shortened dipole antenna whose element length is adjusted to the half-wave length at 80 MHz is used to evaluate the site attenuation of the compact anechoic chamber less than 80 MHz [5], [6].

In this paper, a pair of Schwarzbeck VHAP, whose element diameter is 8 mm, have been used as a shortened dipole antenna less than 80 MHz, and as a half-wave dipole antenna from 80 MHz to 250 MHz. The sub-cell method [7] has been used for the modeling of the dipole antenna. On the calculation, an antenna factor of the dipole antenna depends on an equivalent diameter for the sub-cell method [4]. Therefore, the CSA (Classical Site Attenuation) in free space is calculated by the FDTD method when the cell size is around 40 mm and the equivalent diameter for sub-cell method is changed from 3 mm to 17 mm. The results are then compared with the ones by the method of moment [8]. Its deviation is shown in Fig. 2. From this figure, the optimum equivalent diameters can be determined so that the CSA in free space by the FDTD method coincides with the one by the method of moment.

The optimum equivalent diameters are shown in Fig. 3. This shows that the equivalent diameter changes at the 70 MHz where the antenna changes from the shortened dipole antenna to the half-wave dipole antenna. The optimum equivalent diameters are around 3 mm less than 70 MHz and they are around 16 mm at 80 MHz or more. It might be concerned with the current distribution on the dipole antenna using the large cell. However, the reason has not yet been cleared.

In order to evaluate the validity of the compensation method by the optimum equivalent diameter, the CSA in semi-infinite space has been calculated by the FDTD method from 30 MHz to 250 MHz. Two dipole antennas, whose distance is 3 m, are used and a PML (Perfectly Matched Layer) is applied to present the semi-infinite space.

On the calculation, the CSA_{FDTD} (in dB) is calculated using following equation,

$$CSA_{FDTD} = SA_{FDTD} + \alpha_{TX} + \alpha_{RX} \tag{1}$$

where α_{TX} (in dB) and α_{RX} (in dB) are balun loss of VHAP. The SA_{FDTD} is propagation loss between antennas, which is calculated by the FDTD method. The cell size of around 40 mm is employed for calculation.

The deviation from the VCCI standard [5] to the CSA by the FDTD method is shown in Fig. 4. The calculated values by the FDTD method with the compensation method agree with the VCCI standard within about plus/minus 0.5 dB. The compensation method can be used to model the dipole antenna when we use the large cell to calculate the site attenuation.

2.2 FDTD Modeling of Absorber

The ferrite tile is generally used as absorber of a compact anechoic chamber. Since the cell size is larger than the thickness of the ferrite tile (6.3 mm), the ferrite tile is modeled by the equivalent conversion [4]. However, the absorber of the chamber in Fig. 1 is constructed with the ferrite tile

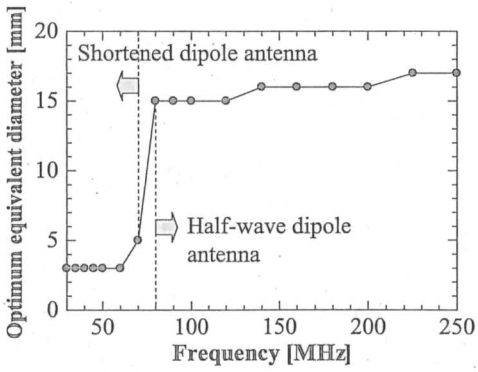

Fig. 3 Calculation results of optimum equivalent diameter.

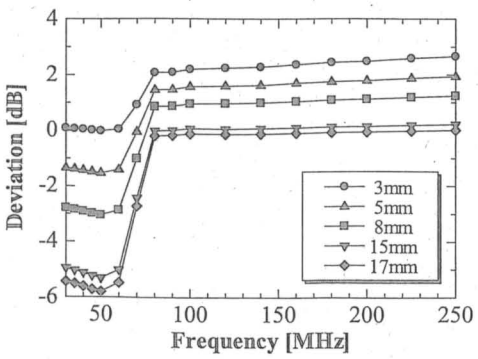

Fig. 2 Deviation of CSA in free space by FDTD and MoM.

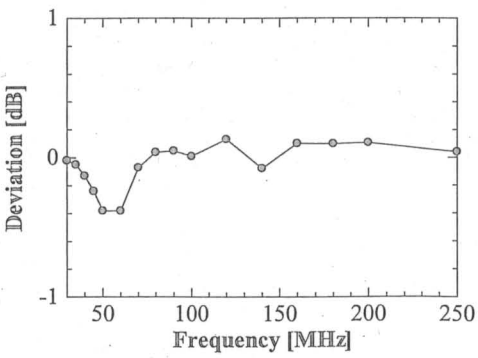

Fig. 4 Deviation from the VCCI standard to calculated results.

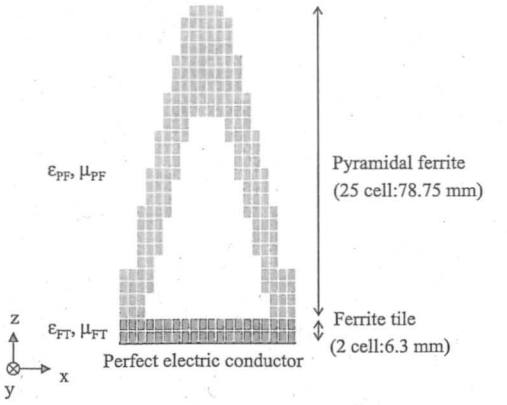

(a) Fine cell ($\Delta x = \Delta y = 2.5$mm, $\Delta z = 3.15$ mm)

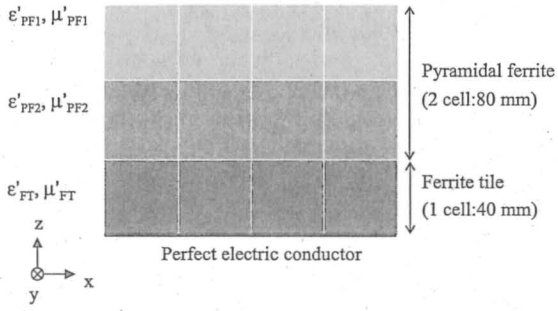

(b) Large cell ($\Delta x = \Delta y = \Delta z = 40$ mm)

Fig. 5 FDTD modeling of absorber using fine cell and large cell.

and the pyramidal ferrite [9]. When the frequency is less than 100 MHz, the pyramidal ferrite does not affect the site attenuation characteristics, because the absorption of the absorber is mostly caused by the ferrite tile. On the other hand, we should estimate the absorption effect of the pyramidal ferrite when the frequency is 100 MHz or more. Thus, the pyramidal ferrite is also modeled using the large cell.

The FDTD modeling of the absorber is shown in Fig. 5. In the fine cell model, the absorber is constructed with the pyramidal ferrite whose height is around 80 mm, and the ferrite tile whose thickness is 6.3 mm.

In the large cell model, three large cells are used. One large cell is used to model the ferrite tile. The equivalent conversion method [4] is used to determine the equivalent dielectric constant and magnetic permeability. Two large cells are used to model the pyramidal ferrite. The equivalent dielectric constant and magnetic permeability are determined from the volume ratio, which is given by (2),

$$\left.\begin{aligned} \varepsilon'_{PFi} &= \frac{V_{AIRi}\varepsilon_0 + V_{PFi}\varepsilon_{PF}}{V_{AIRi} + V_{PFi}} \\ \mu'_{PFi} &= \frac{V_{AIRi}\mu_0 + V_{PFi}\mu_{PF}}{V_{AIRi} + V_{PFi}} \end{aligned}\right\} \quad (i = 1, 2) \qquad (2)$$

where V_{AIR1} and V_{AIR2} are the volume of the upper part and the lower part of air, and V_{PF1} and V_{PF2} are the volume of the upper part and the lower part of a pyramidal ferrite, respectively.

In order to evaluate the validity of the modeling method, the reflection coefficient of the absorber has been

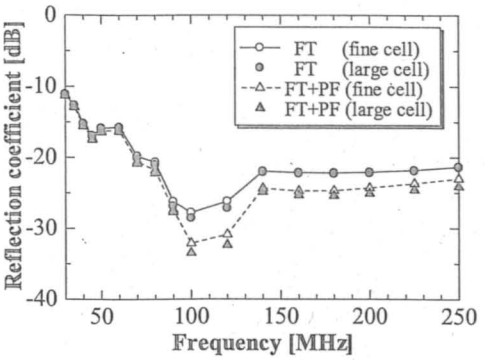

Fig. 6 Reflection coefficient of absorber.

calculated using both the fine cell modeling and the large cell modeling. The dielectric constant and magnetic permeability of the ferrite tile and the pyramidal ferrite have been measured. The fine cell modeling is shown in Fig. 5(a). The cell size is 3.15 mm which is smaller than the thickness of the ferrite tile and is sufficient to present the configuration of the pyramidal ferrite.

The comparison of the calculation results is shown in Fig. 6. On the calculation, the parallel-plate wave-guide model constructed with two perfect conductive plates and the magnetic side walls is used. The plane wave is incident to the absorber. The number of the cell at transverse plane is 4 by 4 for the large cell modeling and 20 by 20 for the fine cell modeling. The number of the cell from the absorber to the signal source is 600 for the large cell modeling and 2000 for the fine cell modeling. The gaussian pulse, whose width is sufficiently shorter to separate between incident wave and reflective wave, is used. The white circles and triangles are the calculated reflection coefficient using the fine cell modeling, and the black circles and triangles are the calculated reflection coefficient using the large cell modeling. This shows that the calculation results using the large cell modeling almost agree with the ones using the fine cell modeling. This means that the large cell modeling can be used to present the absorber shown in Fig. 5(a). In Fig. 6, the circles show the calculation results when we consider only the ferrite tile, and the triangles show the calculation results when we consider both the pyramidal ferrite and the ferrite tile. These calculation results almost agree each other when the frequency is less than 100 MHz. However, it is not identical when the frequency is 100 MHz or more. This means that we should consider the effects of the pyramidal ferrite to calculate the site attenuation when the frequency is 100 MHz or more.

2.3 Site Attenuation by Ray-Tracing Method

The ray-tracing method is widely used to calculate the site attenuation. In this method, the image sources of the transmitting and receiving antenna are determined from the assumption. The reflection of the absorber is considered with the absorption loss when the trace from image sources goes through the wall.

The pyramidal ferrite is modeled using the multi layer plane approximation [2], [10]. In this calculation, the reflection coefficient is obtained based on transmission line equation with sixteen planes, and we considered five times reflections.

3. Comparison of Two Methods

3.1 Measurement of CSA

In order to evaluate the frequency scope of the FDTD method and the ray-tracing method, we compare the measured CSA with the calculated one. The compact anechoic chamber, whose size is 7 m long, 4 m wide, and 3.5 m high, has been used for experiment. The absorber is constructed with the ferrite tile and the pyramidal ferrite [9].

The CSA measurement system is shown in Fig. 7. A pair of VHAP are used for transmitting and receiving antenna as a shortened dipole antenna and a half-wave dipole antenna. They are placed at the distance of 3 m, the height is 1 m and 1.75 m, and the polarization is horizontal and vertical. The measured CSA (in dB) is given in (3), where V_D (in dB) is the received voltage at cable direct connection, and V_{SITE} (in dB) is the one at propagation between antennas.

$$CSA_{MEAS.} = V_D - V_{SITE} \tag{3}$$

3.2 Calculation of CSA

On the FDTD calculation, the model shown in Fig. 1 has been used. The cell size is around 40 mm. The shortened dipole antenna and the half-wave dipole antenna are modeled by the optimum equivalent diameter shown in Fig. 3. The absorbers are modeled using the method described in Sect. 2.2.

It has been also calculated by the ray-tracing method using the method described in Sect. 2.3.

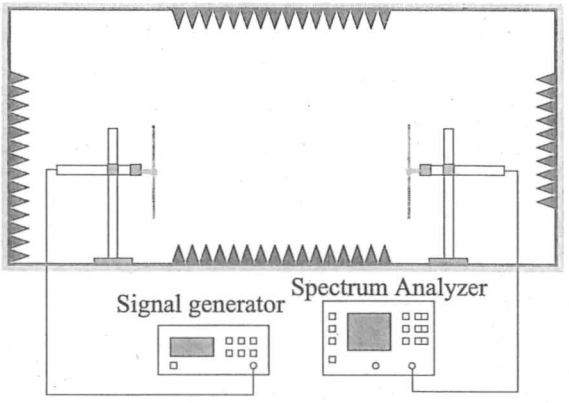

Fig. 7 CSA measurement system.

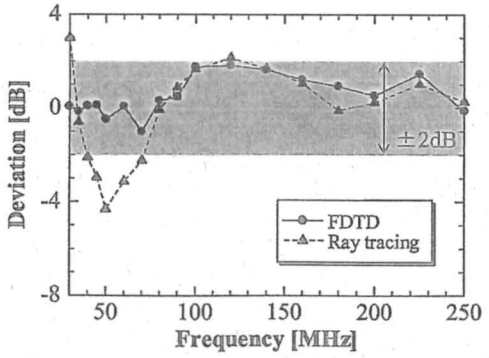

(a) Horizontal polarization (antenna height = 1m)

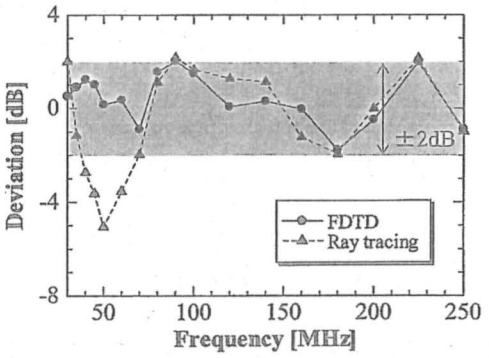

(b) Horizontal polarization (antenna height = 1.75m)

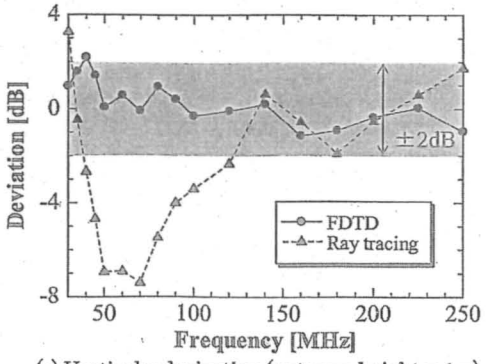

(c) Vertical polarization (antenna height = 1m)

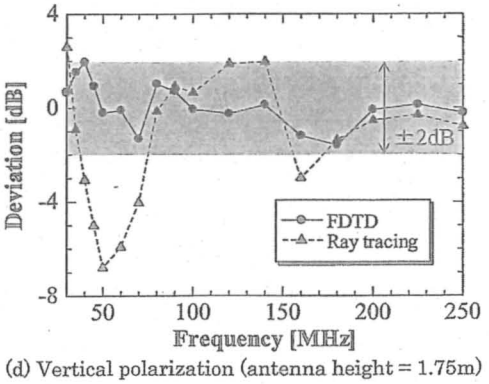

(d) Vertical polarization (antenna height = 1.75m)

Fig. 8 Evaluation results of site attenuation for compact anechoic chamber.

3.3 Evaluation of Two Methods

Figure 8 shows the deviation from the measured CSA to the calculated ones by the FDTD method and the ray-tracing method. From Fig. 8, the following results are obtained;

- The calculated values by the FDTD method agree with the measured ones within plus/minus 2 dB from 30 MHz to 250 MHz.
- The calculated values by the ray-tracing method have larger deviation less than 180 MHz.
- The calculated values by the ray-tracing method almost agree with the ones by the FDTD method at 180 MHz or more.

These results indicate that the FDTD analysis method should be used less than 180 MHz for the chamber in Fig. 1 if we should maintain the deviation within plus/minus 2 dB.

There are several types of chambers and absorbers in the world. So, it needs more investigation to obtain the general relations between the lower frequency limit of the ray-tracing method and the chamber size. However, it is an interesting problem, then we present the evaluation example for the model used in this paper. The result is shown in Fig. 9. We calculated the CSA by both the ray-tracing method and the FDTD method for the two type chambers, whose size were 9 m by 6 m by 5.5 m and 11 m by 8 m by 7.5 m respectively, besides the chamber shown in Fig. 1. Receiving and transmitting antenna are placed at the center positions of chambers, and the polarization of the antenna is vertical. Figure 9 shows the deviation from the FDTD calculation value to the ray-tracing calculation value. Assuming that the allowable deviation is within plus/minus 2 dB, this shows that the lower frequency limit of the ray-tracing method decreases as the chamber size increases.

As shown in Fig. 8, the deviation peak appears at around 50 MHz. Figure 9 shows that the frequency of the deviation peak shifts to lower and the value also decreases when the chamber goes larger. These results suggest that the chamber has the resonance in this frequency range and the ray-tracing method cannot sufficiently present the phenomenon. However, some things, which are the limit of assuming the far field, and etc. affect the deviation. Therefore, the investigation of the deviation reason is a future problem.

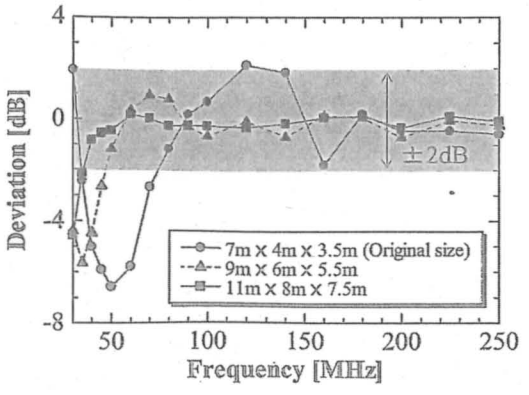

Fig. 9 Deviation from CSA by FDTD to CSA by ray-tracing.

4. Conclusion

In this paper, we investigate the frequency scope of the FDTD method and the ray-tracing method for the site attenuation calculation.

Initially, the FDTD modeling method has been considered when the frequency is more than 100 MHz. The dipole antenna and the absorber are modeled by using large cell whose size is larger than the diameter of the antenna element. In order to compensate the deviation caused by the cell size, the optimum equivalent diameter is determined so that the CSA in free space coincides with the one by the method of moment for the dipole antenna. The absorber is modeled by the three large cells. The equivalent dielectric constant and magnetic permeability are determined by using the equivalent conversion method and the volume ratio.

Then, The CSA of the compact anechoic chamber has been calculated by the FDTD method and the ray-tracing method from 30 MHz to 250 MHz, and they are compared with the measured one. As the results, the calculated values by the FDTD method agree well with the measured ones within plus/minus 2 dB in this frequency range. The calculated values by the ray-tracing method do not agree with the ones by the FDTD method and the measured values when the frequency is less than 180 MHz. This means that the ray-tracing method cannot be applied for the compact anechoic chamber in Fig. 1 when we maintain the deviation from the measured value within plus/minus 2 dB.

Finally, the CSA was calculated by two methods when the chamber size was changed. The result indicates that the larger the chamber size, the lower the frequency limit of the ray-tracing method.

In the future, we plan to investigate the relation between the lower frequency limit of the ray-tracing method and the chamber size for various types chamber.

References

[1] CISPR 16, Specification for radio disturbance and immunity measuring apparatus and methods, Part 1: Radio disturbance and immunity measuring apparatus and Part 2: Methods of measurement of disturbances and immunity.
[2] M. Inoguchi, E. Kimura, and M. Tokuda, "Analyzing and improving characteristics of anechoic chamber using ray tracing method," 4th European Symposium on Electromagnetic Compatibility (EMC Europe 2000 Brugge), vol.1, pp.143–148, Sept. 2000.
[3] A. Taflove and S.C. Hagness, Computational Electrodynamics—The Finite-Difference Time-Domain Method, second ed., Artech House Publishers, 2000.
[4] M. Kawabata, Y. Ishida, K. Shimada, A. Kitani, and N. Kuwabara, "Evaluation of site attenuation of fully compact anechoic chamber using FDTD method," IEICE Technical Report, EMCJ2002-108, Jan. 2003.
[5] http://www.vcci.or.jp/
[6] A. Maeda, A. Sugiura, N. Kuwabara, and S. Usuda, "Site attenuation measurements using shortened dipole antennas," IEICE Trans. Commun. (Japanese Edition), vol.J79-B-II, no.11, pp.764–770, Nov.

1996.
[7] K.R. Umashankar, A. Taflove, and B. Beker, "Calculation and experimental validation of induced currents on coupled wires in an arbitrary shaped cavity," IEEE Trans. Antennas Propag., vol.35, no.11, pp.1248–1257, Nov. 1987.
[8] G.J. Burke and A.J. Poggio, Numerical Electromagnetics Code (NEC)—Method of Moments, Lawrence Livermore Laboratory, 1981.
[9] K. Shimada, M. Tosa, Y. Ishida, and M. Tokuda, "Characteristic of fully compact anechoic chamber using pyramidal ferrite absorber," IEICE Technical Report, EMCJ2002-12, May 2002.
[10] H. Anzai, Y. Naito, and T. Mizumoto, "Characteristics of pyramidal electromagnetic wave absorber for oblique incidence and its equivalent representation used by the approximate method," IEICE Trans. Commun. (Japanese Edition), vol.J79-B-II, no.10, pp.686–693, Oct. 1996.

Masato Kawabata received the B.S. degree in Electrical Engineering and the M.S. degree in Electronics and Information Engineering from Hokkaido University in 1995 and 1997, respectively. He joined Kawasaki Heavy Industries, Ltd, in 1997. He joined Fukuoka Industrial Technology Center, Mechanics and Electronics Research Institute in 2002. He presently is engaged in research of EMI measurement and evaluation of anechoic chamber.

Yasuhiro Ishida received the B.S. and M.S. degrees in Electrical Engineering from Kyushu University in 1986 and 1988, respectively. He joined Kyushu Matsushita Electric Co., Ltd., in 1988. He joined Fukuoka Industrial Technology Center, Mechanics and Electronics Research Institute in 1992. Since then, he has been engaged in research and development of EMI measurement and suppression, and he received the Ph.D. degree from Kyushu Institute of Technology in 2001. His current research interests include the radiated emission sources finding technique. He is a member of IEEE.

Kazuo Shimada received the B.S. degree in Electrical Engineering from Chiba Institute of Technology in 1988. In that year, he joined in Akzo Kashima, Ltd. He joined Riken Eletech Co., Ltd., in 1992. Since then, he has been engaged in research and development of EM absorber and anechoic chamber.

Nobuo Kuwabara received the B.E. and M.E. degrees in Electronic Engineering from Shizuoka University in 1975 and 1977, respectively. He also holds the Ph.D. degree in Engineering from Shizuoka University, granted in 1992. Since joining NTT in 1977, he had been researching over-voltage protection of telecommunication systems, designing induction-free optical-fiber cables and electromagnetic compatibility in electro-communication systems. At present, he is a professor in the faculty of engineering, Kyushu Institute of Technology. He is a member of IEEE.